Progress In Electromagnetics Research, Vol. 120, 143–164, 2011

INVESTIGATIONS OF CYLINDRICAL FERRITE COUPLED LINE JUNCTION USING HYBRID TECHNIQUE

A. Kusiek*, W. Marynowski, and J. Mazur

Faculty of Electronics, Telecommunications and Informatics, Gdansk University of Technology, Gdansk, Poland

Abstract—In this paper, a novel longitudinally magnetized cylindrical ferrite coupled line (CFCL) junction is proposed. In comparison to planar ferrite coupled line (FCL) configurations, which are well known in literature, in such structure the higher gyromagnetic coupling occurs. This allows to obtain the required in FCL devices Faraday rotation angle $\pi/4$ for the ferrite with shorter length and lower value of magnetization. As a result the total insertion losses in the ferrite section can be reduced using the proposed topology. In the analysis of the proposed CFCL junction a hybrid technique combining method of moments and coupled mode method (MoM/CMM) is applied. The results are compared with the ones obtained from commercial software HFSS and a good agreement is obtained.

1. INTRODUCTION

Nonreciprocal devices have been extensively used in modern microwave and millimeter systems [1–16]. In order to obtain the nonreciprocal effects one needs to utilize the ferrite materials [1–15] or active elements such as amplifiers [16]. Recently, the longitudinally magnetized ferrite coupled strip-[2, 4–10, 15, 17, 18] or slotlines [14, 19] are being developed and employed to realize integrated nonreciprocal devices. Significant interest in these devices results from their advantages which are weak biasing magnetic field and wide operation bandwidth [6, 10].

The basic part of ferrite coupled line (FCL) devices is longitudinally magnetized FCL section obtained as a section of two coupled lines placed on ferrite substrate [1–3]. According to the

Received 27 July 2011, Accepted 22 August 2011, Scheduled 3 September 2011

* Corresponding author: Adam Kusiek (adakus@eti.pg.gda.pl).

coupled-mode model [1] in such section the gyromagnetic coupling occurs resulting in Faraday rotation effect. The wide operation bandwidth and high isolation is obtained, when the Faraday rotation phenomenon is optimal. This optimal effect is achieved when the ferrite material is placed in the region where the wave is linearly polarized and occurs in cylindrical waveguide with coaxially located ferrite rod or suspended stripline junction. In order to construct devices such as circulators [7, 19], gyrators [20] or isolators [17] the FCL section has to be cascaded with reciprocal section providing input signals to the FCL which are either in phase or out of phase.

So far, studies concerning FCL devices have been focused mainly on structures realized in planar line technology [19, 21]. Such structures allow one to obtain fully integrated FCL devices. However, due to the significant length of ferrite section, the main drawbacks are high insertion losses occurring in ferrite material and large dimensions of the structure. Also due to the geometry of line in planar junction it is difficult to obtain a linear polarization of the wave and to eliminate the isotropic coupling which results in significant deterioration of isolation.

There were several attempts to improve performance and to reduce total dimensions of planar FCL devices. Promising results concerning low insertion losses and high isolation were obtained for the nonreciprocal devices employing ferrite coupled slotline [19] and stripline junctions [2, 7]. For the fabricated devices obtained insertion losses were not lower than 3dB and isolation was better than 12 dB [7, 15, 19]. Moreover in order to reduce the dimensions of the planar FCL devices in [8] the circulator with appropriate matching networks at the ports ensuring multiple reflections was proposed. For presented device the FCL junction length reduction by a factor of two was obtained. The drawback of this structure was high value of insertion losses caused by multiple transmission of signal through the lossy ferrite junction. Also similar length reduction of FCL junction was achieved with the use of periodic left-handed/ferrite coupled line (LH-FCL) structures [22, 23]. However, for the simulated circulator utilizing LH-FCL section the insertion losses were not better than 4 dB.

Due to the high insertion losses and low level of isolation there is still need for developing novel FCL junctions offering better performance than currently proposed planar configurations. In this paper, we propose for the first time a cylindrical ferrite coupled line junction (CFCL). Due to the similar geometry to the circular waveguide with coaxially located ferrite rod such structure allows to obtain close to optimal Faraday rotation effect. Moreover, in such configuration stronger gyromagnetic coupling occurs which is a result of high magnetic field concentration in the ferrite medium.

These make possible to design shorter ferrite junctions ensuring lower insertion losses and better performance, e.g., better isolation and wider operation bandwidth in comparison to planar ones.

In the analysis of the proposed structure the hybrid technique combining method-of-moment (MoM) with coupled-mode method (CMM) [24, 25] is applied. The analysis using MoM/CMM involves introducing an isotropic basic guide. This guide is complementary to the ferrite one, however instead of ferrite the dielectric characterized by scalar value of $\mu_r = 1$ is used. In this approach the basic guide modes obtained from MoM are used to determine the ferrite modes of the investigated structure. As a result of analysis the dispersion characteristics of ferrite line, the gyromagnetic coupling coefficients and the scattering parameters of ferrite junction are obtained. The presented results are compared with the commercial software HFSS. A good agreement between presented results and the reference ones is obtained.

2. FORMULATION OF THE PROBLEM

The proposed four-port CFCL junction is presented in Fig. 1. It consists of a cascade connection of two dielectric and ferrite loaded coupled transmission lines, where the ferrite is magnetized longitudinally. In order to determine wave properties (e.g., dispersion characteristics, gyromagnetic coupling factor) and scattering parameters of the considered structure we utilize the hybrid MoM/CMM technique. In this approach at first the propagation coefficients and field distributions of modes in a basic cylindrical dielectric coupled line (CDCL) are determined with the use of MoM (see Section 2.1). This guide has the same cross section as CFCL, where instead of ferrite the dielectric rod with the same permittivity and relative permeability $\mu_r = 1$ is applied. In our analysis we take into considerations only two propagated fundamental basic modes whereas higher ones such as evanescent modes are neglected. Next, utilizing CMM the dispersion characteristics of two basic modes in ferrite guide, the gyromagnetic coupling coefficient and scattering parameters of CFCL junction are calculated (see Section 2.2). It should be noted that proposed model allows one for fast and accurate determination of an optimal length of CFCL section. Moreover, having calculated scattering matrix of such junction, it can be easily used to predict the behavior of nonreciprocal devices, e.g., isolators and circulators employing proposed ferrite coupled line junction [19, 25].

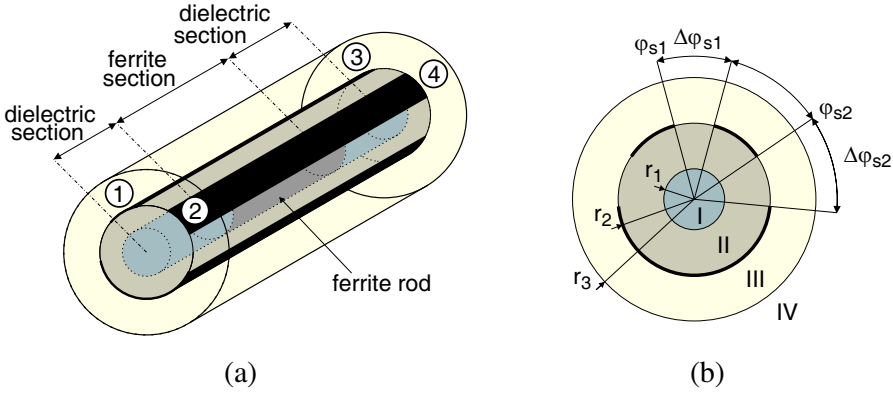

Figure 1. Cylindrical ferrite coupled line junction (CFCL): (a) 3D-view and (b) cross-section.

2.1. Cylindrical Dielectric Coupled Line

The cross-section of considered line is presented in Fig. 1(b). The longitudinal components of electric and magnetic fields in each region take the following form:

$$E_z^l = \sum_{m=-M}^{M} \left(A_{1m}^{E,\,l} R_m^{(1)}(k_{\rho l}\rho) + A_{2m}^{E,\,l} R_m^{(2)}(k_{\rho l}\rho) \right) e^{jm\varphi} e^{-j\beta z}, \quad (1)$$

$$H_z^l = \frac{j}{\eta_l} \sum_{m=-M}^{M} \left(A_{1m}^{H,\,l} R_m^{(1)}(k_{\rho l}\rho) + A_{2m}^{H,\,l} R_m^{(2)}(k_{\rho l}\rho) \right) e^{jm\varphi} e^{-j\beta z}. \quad (2)$$

where $\omega = \frac{2\pi f}{c}$, $k_{\rho l} = \sqrt{k_l^2 - \beta^2}$, $k_l = \frac{\omega\sqrt{\mu_l \varepsilon_l}}{c}$, $\eta_l = \sqrt{\frac{\mu_l}{\varepsilon_l}}$, μ_l and ε_l denote permeability and permittivity in lth region, respectively. In above equations $R_m^{(1)}(\cdot)$ and $R_m^{(2)}(\cdot)$ denote two linearly independent radial cylindrical functions and depending on the region they are defined as follows:

region 1	$R_m^{(1)}(\cdot) = J_m(\cdot)$, $R_m^{(2)}(\cdot)$ — neglected	
region 2, 3	$R_m^{(1)}(\cdot) = J_m(\cdot)$, $R_m^{(2)}(\cdot) = Y_m(\cdot)$	
region 4	$R_m^{(1)}(\cdot) = J_m(\cdot)$, $R_m^{(2)}(\cdot) = Y_m(\cdot)$	— shielded guide
	$R_m^{(1)}(\cdot)$ — neglected, $R_m^{(2)}(\cdot) = H_m^{(2)}(\cdot)$	— open guide

where J_m, Y_m and $H_m^{(2)}$ are mth order Bessel, Neumann and Hankel function of second kind, respectively. Utilizing (1) and (2) the transverse electric and magnetic fields components can be found

directly from Maxwell's equations [26]. Now, in order to determine the propagation coefficient β and field distributions in the considered guide we utilize the continuity conditions of z and φ field components in the boundaries between neighboring regions. At first we use the boundary continuity conditions between regions 1-2 ($\rho = r_1$) and 3-4 ($\rho = r_3$):

$$E^n_{z,\varphi}(r_n, \varphi) = E^{n+1}_{z,\varphi}(r_n, \varphi), \tag{3}$$

$$H^n_{z,\varphi}(r_n, \varphi) = H^{n+1}_{z,\varphi}(r_n, \varphi), \tag{4}$$

where $n = 1, 3$ and $\varphi \in [0, 2\pi]$. Applying the orthogonality properties of $e^{jm\varphi}$ to Equations (3) and (4) we obtain relation between coefficients $A^{(\cdot),2}_{1m}$, $A^{(\cdot),2}_{2m}$ and $A^{(\cdot),3}_{1m}$, $A^{(\cdot),3}_{2m}$, respectively in a form:

$$\mathbf{A}^2_2 = \mathbf{T}_2\mathbf{A}^2_1 \quad \text{and} \quad \mathbf{A}^3_1 = \mathbf{T}_3\mathbf{A}^3_2,$$

where $\mathbf{A}^l_p = [A^{E,\,l}_{p(-M)}, \ldots, A^{E,\,l}_{pM}, A^{H,\,l}_{p(-M)}, \ldots, A^{H,\,l}_{pM}]^T$ and

$$\mathbf{T}_2 = \left(\mathbf{Z}_1\mathbf{M}^{H,2}_{A2} - \mathbf{M}^{E,2}_{A2}\right)^{-1}\left(\mathbf{M}^{E,2}_{A1} - \mathbf{Z_1}\mathbf{M}^{H,2}_{A1}\right), \tag{5}$$

$$\mathbf{T}_3 = \left(\mathbf{Z}_4\mathbf{M}^{H,3}_{A1} - \mathbf{M}^{E,3}_{A1}\right)^{-1}\left(\mathbf{M}^{E,3}_{A2} - \mathbf{Z_1}\mathbf{M}^{H,3}_{A2}\right), \tag{6}$$

$$\mathbf{Z}_l = \mathbf{M}^{E,l}_{A1}\left(\mathbf{M}^{H,l}_{A1}\right)^{-1} \quad \text{for} \quad l = 1, 4. \tag{7}$$

For the sake of brevity matrices $\mathbf{M}^{E,\cdot}_{A1}$, $\mathbf{M}^{H,\cdot}_{A1}$, $\mathbf{M}^{E,\cdot}_{A2}$ and $\mathbf{M}^{H,\cdot}_{A2}$ are defined in Appendix A.

Next, we consider the boundary between regions 2 and 3. In order to include in the analysis the metallization layer at first we define z and φ components of electric field at $\rho = r_2$. These electric field is non-zero in each ith slot area of the line and is expressed as follows:

$$E^s_z = \sum_{i=1}^{I}\sum_{k=1}^{K} A^s_k \sin\left(\frac{\varphi - \varphi_{si}}{\Delta\varphi_{si}} k\pi\right), \tag{8}$$

$$E^s_\varphi = \sum_{i=1}^{I}\sum_{k=0}^{K} A^s_k \cos\left(\frac{\varphi - \varphi_{si}}{\Delta\varphi_{si}} k\pi\right), \tag{9}$$

where $\varphi_i \in [\varphi_{si}, \varphi_{si} + \Delta\varphi_{si}]$ and I denotes a number of slots in the considered guide. By applying the boundary continuity conditions between electric fields in regions 2, 3 and in the slots area:

$$E^l_z(r_l, \varphi) = E^s_z(r_l, \varphi), \tag{10}$$

$$E^l_\varphi(r_l, \varphi) = E^s_\varphi(r_l, \varphi) \quad \text{for} \quad l = \{2, 3\} \tag{11}$$

and utilizing orthogonality of $e^{jm\varphi}$ we obtain the following set of equations:

$$\mathbf{A}_1^2 = \left[\left(\mathbf{M}_{A1}^{E,2} + \mathbf{M}_{A2}^{E,2}\mathbf{T}_{12}\right)\right]^{-1} \mathbf{I}_{os}\mathbf{A}_s, \tag{12}$$

$$\mathbf{A}_2^3 = \left[\left(\mathbf{M}_{A1}^{E,3}\mathbf{T}_{34} + \mathbf{M}_{A2}^{E,3}\right)\right]^{-1} \mathbf{I}_{os}\mathbf{A}_s, \tag{13}$$

where $\mathbf{I}_{os}$ is a matrix of integrals defined in Appendix A. Finally, we enforce the continuity of z and φ components of magnetic field from regions 2 and 3 in the slot areas of line:

$$H_z^2(r_2, \varphi_i) = H_z^3(r_2, \varphi_i), \tag{14}$$

$$H_\varphi^2(r_2, \varphi_i) = H_\varphi^3(r_2, \varphi_i), \tag{15}$$

where $\varphi_i \in [\varphi_{si}, \varphi_{si}+\Delta\varphi_{si}]$. Using basis functions (8) and (9) as testing functions to solve (15) and (14), respectively and applying relations (12) and (13) to resulting set of equations we obtain:

$$\mathbf{D}\mathbf{A}_s = 0, \tag{16}$$

where

$$\mathbf{D} = \mathbf{I}_{so}\left[\mathbf{M}^{H,3}\left(\mathbf{M}^{E,3}\right)^{-1} - \mathbf{M}^{H,2}\left(\mathbf{M}^{E,2}\right)^{-1}\right]\mathbf{I}_{os} \tag{17}$$

and $\mathbf{M}^{E,(\cdot)}$, $\mathbf{M}^{H,(\cdot)}$, $\mathbf{I}_{so}$ are defined in Appendix A. Solving Equation (16) the propagation coefficients β and distributions of electric $\mathbf{E}$ and magnetic $\mathbf{H}$ modal fields in the considered cylindrical dielectric guide are obtained.

2.2. Cylindrical Ferrite Coupled Line

Applying solution of (16) to coupled-mode method (CMM) a gyromagnetic coupling coefficients, propagation coefficients of ferrite modes and scattering matrix of CFCL junction can be determined [3, 11, 27]. In this approach the transversal electric and magnetic fields in the investigated ferrite guide are expressed in terms of basic guide field eigenfunctions $\mathbf{e}_{t,e(o)}$ and $\mathbf{h}_{t,e(o)}$ as follows:

$$\mathbf{E}_t^f = \widehat{U}_e(z)\mathbf{e}_{t,e} + \widehat{U}_o(z)\mathbf{e}_{t,o}, \tag{18}$$

$$\mathbf{H}_t^f = \widehat{I}_e(z)\mathbf{h}_{t,e} + \widehat{I}_o(z)\mathbf{h}_{t,o}. \tag{19}$$

In above equations subscripts e and o denote even and odd mode, $\widehat{U}_{e(o)}(z) = \widehat{U}_{e(o)}\mathrm{e}^{-\mathrm{j}kz}$ and $\widehat{I}_{e(o)}(z) = \widehat{I}_{e(o)}\mathrm{e}^{-\mathrm{j}kz}$ are modal voltage and current, k is the unknown propagation coefficient in ferrite guide and eigenfunctions $\mathbf{e}_{t,e(o)}$ and $\mathbf{h}_{t,e(o)} = -\mathbf{i}_z \times \mathbf{e}_{t,e(o)}$ are normalized as follows:

$$\iint_S \mathbf{e}_{t,e(o)} \times \mathbf{h}_{t,e(o)}\vec{ds} = 1. \tag{20}$$

The Maxwell's equations defined for CDCL and CFCL are combined together and after some mathematical manipulations we obtain similar to [3, 27] set of coupled mode equations defining equivalent transmission line problem of CFCL:

$$\begin{aligned}
&\frac{\partial}{\partial z}\widehat{U}_e(z) + \mathrm{j}\beta_e Z_e \widehat{I}_e(z) = C_{eo}\widehat{I}_o(z),\\
&\frac{\partial}{\partial z}\widehat{U}_o(z) + \mathrm{j}\beta_o Z_o \widehat{I}_o(z) = C_{oe}\widehat{I}_e(z),\\
&\frac{\partial}{\partial z}\widehat{I}_e(z) + \mathrm{j}\beta_e Y_e \widehat{U}_e(z) = 0,\\
&\frac{\partial}{\partial z}\widehat{I}_o(z) + \mathrm{j}\beta_o Y_o \widehat{U}_o(z) = 0,
\end{aligned} \tag{21}$$

where:

$$\begin{aligned}
C_{eo} &= k_0\eta_0\mu_a \int_{\Omega_f} \left(\mathbf{h}_{t,e} \times \mathbf{h}^*_{t,o}\right)\cdot \mathbf{i}_z \,\mathrm{d}\Omega_f,\\
C_{oe} &= -C^*_{eo}
\end{aligned} \tag{22}$$

define the coupling between two fundamental modes in basic guide, Ω_f is a ferrite area in the cross section. Taking into account that in such type of structures the field distributions of the basic modes $\mathbf{E}_{t,e(o)}$ and $\mathbf{H}_{t,e(o)}$ in cross-section of the dielectric guide are much easier determined than eigenfunctions $\mathbf{h}_{t,e(o)}$ and $\mathbf{e}_{t,e(o)}$, we introduce the following relation between fields and eigenfunctions in the dielectric CDCL guide:

$$\mathbf{E}_{t,e(o)} = \overline{U}_{e(o)}(z)\mathbf{e}_{t,e(o)}, \tag{23}$$

$$\mathbf{H}_{t,e(o)} = \overline{I}_{e(o)}(z)\mathbf{h}_{t,e(o)}, \tag{24}$$

where $\overline{U}_{e(o)}(z)$, $\overline{I}_{e(o)}(z)$ are modal voltage and current in the dielectric basic guide. Then, assuming that the power of even and odd mode is defined as:

$$P_{e(o)} = \iint\limits_S \mathbf{E}_{t,e(o)} \times \mathbf{H}^*_{t,e(o)}\mathbf{ds} \tag{25}$$

and the impedance of even and odd mode is:

$$Z_{e(o)} = \frac{\overline{U}_{e(o)}}{\overline{I}_{e(o)}} = \frac{k_0\eta_0}{\beta_{e(o)}}, \tag{26}$$

the coupling coefficient (22) can be formulated as:

$$C_{eo} = k_0\eta_0\mu_a \frac{\sqrt{Z_e Z_o}}{\sqrt{P_e P_o}} \int_{\Omega_f} \left(\mathbf{H}_{t,e} \times \mathbf{H}^*_{t,o}\right)\cdot \mathbf{i}_z \,\mathrm{d}\Omega_f, \tag{27}$$

where $\eta_0 = \sqrt{\mu_0/\varepsilon_0}$ and $\beta_{e(o)}$ are propagation coefficients of two fundamental modes in dielectric guide. The components $\mathbf{H}_{t,e(o)} = H_{\rho,e(o)}\mathbf{i}_\rho + H_{\varphi,e(o)}\mathbf{i}_\varphi$ and $\mathbf{E}_{t,e(o)} = E_{\rho,e(o)}\mathbf{i}_\rho + E_{\varphi,e(o)}\mathbf{i}_\varphi$ are transverse even and odd electric and magnetic modal fields obtained from (16). Equation (27) indicates that the gyromagnetic coupling occurs when the ferrite is located in the area of line where the magnetic field vectors of two basic isotropic modes are orthogonal.

The defined above transmission line model of the ferrite guide can be used to determine scattering matrix of CFCL junction. At first utilizing symmetry properties of the investigated structure the modal even/odd voltage and current can be related to voltage and current defined for each of two coupled lines (see Fig. 2) as follows:

$$\widehat{U}_e(z) = \widehat{U}_1(z) + \widehat{U}_2(z), \qquad \widehat{I}_e(z) = \widehat{I}_1(z) + \widehat{I}_2(z),$$
$$\widehat{U}_o(z) = \widehat{U}_1(z) - \widehat{U}_2(z), \qquad \widehat{I}_o(z) = \widehat{I}_1(z) - \widehat{I}_2(z).$$

Next, applying the above relations to (21) we obtain the eigenvalue problem of the following form:

$$\mathbf{QK} = \mathbf{Kk}, \tag{28}$$

which solution are the eigenvalues k_1 and k_2 defining propagation coefficients of two fundamental modes in ferrite guide. For the sake of brevity matrix $\mathbf{Q}$, diagonal matrix of eigenvalues $\mathbf{k}$ and matrix of eigenvectors $\mathbf{K}$ are defined in Appendix B.

Using the solution of (28) the voltage and current in each of two

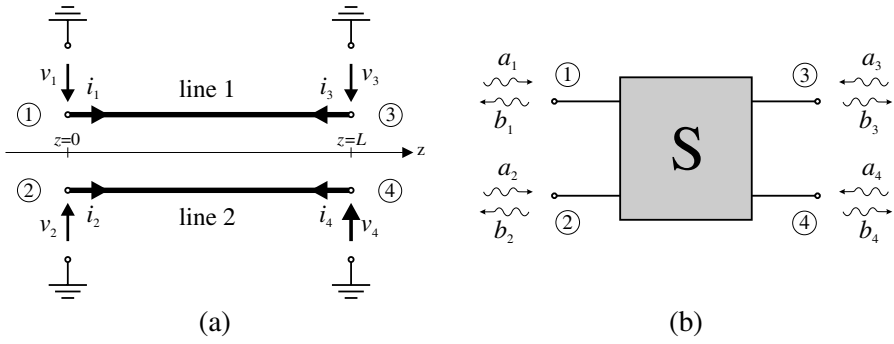

Figure 2. Four-port FCL junction: (a) circuit model, (b) network representation.

coupled lines can be defined at considered z cross-section as follows:

$$\begin{bmatrix} \widehat{U}_1(z) \\ \widehat{U}_2(z) \\ \widehat{I}_1(z) \\ \widehat{I}_2(z) \end{bmatrix} = \mathbf{K} \begin{bmatrix} e^{-\mathrm{j}k_1 z} & 0 & 0 & 0 \\ 0 & e^{\mathrm{j}k_1 z} & 0 & 0 \\ 0 & 0 & e^{-\mathrm{j}k_2 z} & 0 \\ 0 & 0 & 0 & e^{\mathrm{j}k_2 z} \end{bmatrix} \begin{bmatrix} A_1^+ \\ A_1^- \\ A_2^+ \\ A_2^- \end{bmatrix}, \tag{29}$$

where $A_1^{+(-)}$ and $A_2^{+(-)}$ are unknown amplitudes of the forward and backward partial waves in the equivalent transmission line. Assuming notation from Fig. 2(a) and utilizing (29) we can write the relations between voltage and current in the ports of the considered junction defined at interfaces $z = 0$ and $z = L$:

$$\begin{bmatrix} \widehat{U}_1(z) \\ \widehat{U}_2(z) \\ \widehat{I}_1(z) \\ \widehat{I}_2(z) \end{bmatrix}_{z=0} = \begin{bmatrix} v_1 \\ v_2 \\ i_1 \\ i_2 \end{bmatrix} \quad \text{and} \quad \begin{bmatrix} \widehat{U}_1(z) \\ \widehat{U}_2(z) \\ \widehat{I}_1(z) \\ \widehat{I}_2(z) \end{bmatrix}_{z=L} = \begin{bmatrix} v_3 \\ v_4 \\ -i_3 \\ -i_4 \end{bmatrix}. \tag{30}$$

Combining Equations (29) and (30) we obtain the following relation:

$$\begin{bmatrix} v_3 \\ v_4 \\ -i_3 \\ -i_4 \end{bmatrix} = \mathbf{K} \begin{bmatrix} e^{-\mathrm{j}k_1 L} & 0 & 0 & 0 \\ 0 & e^{\mathrm{j}k_1 L} & 0 & 0 \\ 0 & 0 & e^{-\mathrm{j}k_2 L} & 0 \\ 0 & 0 & 0 & e^{\mathrm{j}k_2 L} \end{bmatrix} \mathbf{K}^{-1} \begin{bmatrix} v_1 \\ v_2 \\ i_1 \\ i_2 \end{bmatrix}. \tag{31}$$

Finally, we define incident and reflected waves in each ith port of the structure:

$$a_i = \frac{v_i}{\sqrt{Z_0}} + i_i\sqrt{Z_0} \qquad \text{and} \qquad b_i = \frac{v_i}{\sqrt{Z_0}} - i_i\sqrt{Z_0},$$

where Z_0 is a wave impedance of the port. Applying above relations to (31) we obtain the scattering matrix of four-port CFCL junction which is defined as follows:

$$\begin{bmatrix} b_1 \\ b_2 \\ b_3 \\ b_4 \end{bmatrix} = \begin{bmatrix} S_{11} & S_{12} & S_{13} & S_{14} \\ S_{21} & S_{22} & S_{23} & S_{24} \\ S_{31} & S_{32} & S_{33} & S_{34} \\ S_{41} & S_{42} & S_{43} & S_{44} \end{bmatrix} \begin{bmatrix} a_1 \\ a_2 \\ a_3 \\ a_4 \end{bmatrix}. \tag{32}$$

Assuming instead of the voltage and current waves the real voltage and current distribution in the proposed transmission line model of CFCL junction, the wave impedances $Z_{e(o)}$ and Z_0 can be treated as characteristic impedances.

3. NUMERICAL RESULTS

In the numerical calculation CFCL junction presented in Fig. 1(a) is taken into account. In Section 3.1, parametric studies of the investigated structure are presented. In Section 3.2 the CFCL junction with Faraday rotation angle $\pi/4$ is designed and applied to realize circulator.

3.1. Wave Properties of CFCL Junction

The fabrication process of the proposed CFCL junction from Fig. 1(a) based on metallization etching on cylinder is quite difficult. However such structure can be easily fabricated by etching the circuit on thin dielectric planar substrate and then folding on a dielectric/ferrite circular cylinder.

According to above fabrication constraints in the analysis we assume the CFCL junction with following parameters of ferrite rod: $r_1 = 2.2\,\text{mm}$, $\varepsilon_{rf} = 15.04$, saturation magnetization $M_s = 1800\,\text{Gs}$, internal bias $H_i = 0$, resonance line width $\Delta H = 0$ and dielectric coating: $h_d = r_2 - r_1 = 0.127\,\text{mm}$, $\varepsilon_{rd} = 2.2$ (Taconic TLY-5), angular slots spacing: $\varphi_{s1} = -30°$, $\Delta\varphi_{s1} = 60°$, $\varphi_{s2} = 85°$, $\Delta\varphi_{s2} = 70°$. For the simulation of the presented examples the following numbers of eigenfunctions $M = 30$ and $K = 5$ were assumed in our approach. Utilizing MoM the normalized dispersion characteristics ($\widetilde{\beta}_{e(o)} = \beta_{e(o)}/k_0$) and magnetic field distributions for two basic modes

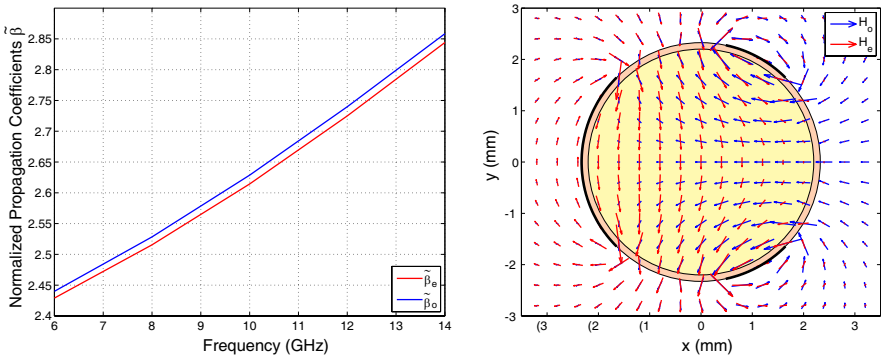

Figure 3. Wave parameters of fundamental even and odd mode in CDCL: (a) normalized dispersion characteristics and (b) transverse magnetic field distributions at $f_0 = 10\,\text{GHz}$.

(even and odd) in CDCL are calculated and presented in Figs. 3(a) and 3(b), respectively. From Fig. 3(b), it can be noticed that in the proposed guide there exists region where magnetic fields of two basic modes are perpendicular to each other. Since, the ferrite material is located in such region, the gyromagnetic coupling occurs (see Equation (27)). Moreover, one can see from Fig. 4, that with the increase of frequency the field is more concentrated in region 1, resulting in increasing of gyromagnetic coupling coefficient.

The parametric studies of gyromagnetic coupling versus parameters of the line are presented in Fig. 5. In Fig. 5(a), the frequency dependent characteristics of normalized gyromagnetic coupling coefficient $\widetilde{C}_{eo} = C_{eo}/(k_0\eta_0\mu_a\sqrt{Z_eZ_o})$ determined for different angular slot $\Delta\varphi_{s1}$ and strip $\Delta\varphi_m$ widths are presented. It can be found that with increasing value of $\Delta\varphi_{s1}$ and $\Delta\varphi_m$ the normalized gyromagnetic coupling coefficient $\widetilde{C}_{eo}$ is also increasing. In Fig. 5(b), the parametric characteristics of $\widetilde{C}_{eo}$, determined in a function of radius of ferrite rod and for different height h_d and permittivity ε_{rd} of dielectric coating, are presented. It can be noticed that $\widetilde{C}_{eo}$ increases with the increase of ferrite rod radius and coating height which results from higher field

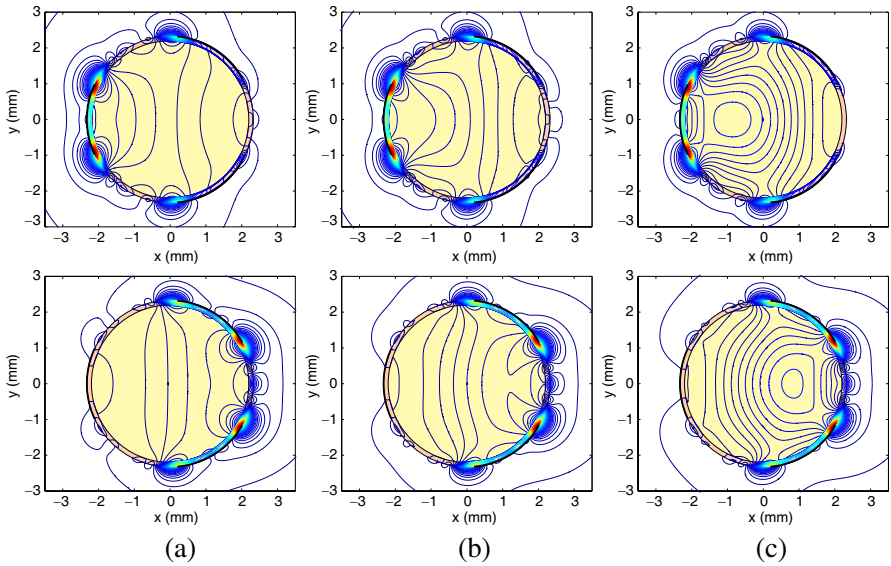

Figure 4. Poynting vector distribution of fundamental even and odd mode in CDCL at frequency: (a) $f_0 = 7\,\text{GHz}$, (b) $f_0 = 10\,\text{GHz}$ and (c) $f_0 = 13\,\text{GHz}$.

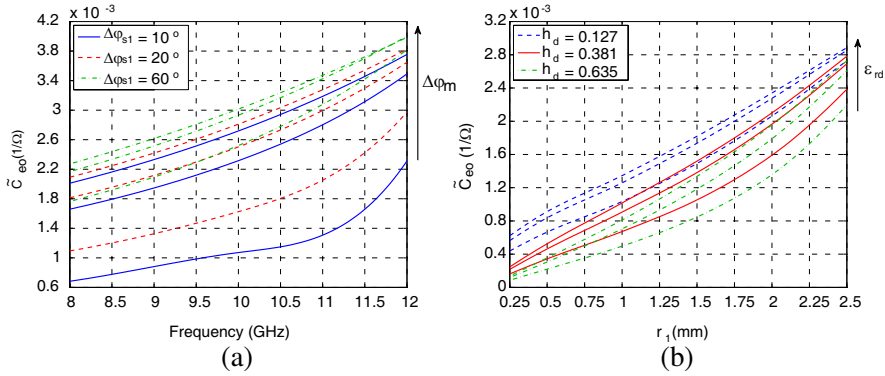

Figure 5. Characteristics of normalized gyromagnetic coupling coefficient $\widetilde{C}_{eo}$ versus: (a) frequency for different slot $\Delta\varphi_{s1}$ and strip $\Delta\varphi_m$ angular widths, (b) radius of ferrite rod for different height $h_d = r_2 - r_1$ and permittivity ε_{rd} of the coating at $f_0 = 8\,\mathrm{GHz}$. Parameters: $\Delta\varphi_m = \varphi_{s2} - \varphi_{s1} - \Delta\varphi_{s1} = \{10, 30, 50\}\,\mathrm{deg}$ and $= \varepsilon_{rd} = \{2.2, 4.5, 6\}$.

concentration in the ferrite rod. On the other hand with the increasing value of dielectric permittivity ε_{rd}, the field becomes to concentrate in the coat, hence the gyromagnetic coupling decreases.

Utilizing calculated gyromagnetic coupling coefficients from Figs. 5(a) and 5(b) and propagation coefficients of even and odd mode the normalized dispersion characteristics of ferrites modes are calculated from relation (B2) and presented in Fig. 6. In Figs. 6(a), 6(b) and Figs. 6(c), 6(d) the normalized propagation coefficients of two ferrite modes ($\widetilde{k}_{1(2)} = k_{1(2)}/k_0$) are shown, respectively. Moreover, in Figs. 6(e) and 6(f) the difference between calculated propagation coefficients is depicted, which can be used to determine the approximate length of ferrite section ensuring Faraday rotation angle $\pi/4$ [28] as follows:

$$L^a_{opt} = \frac{\pi}{2(k_1 - k_2)}. \tag{33}$$

In the case of angular variation of slots and strips one can observe that despite the increase of coupling coefficient with the increasing values of $\Delta\varphi_{s1}$ and $\Delta\varphi_m$, the difference between propagation coefficients is decreasing (see Fig. 6(e)). The opposite effect is observed with the variation of height h_d and permittivity ε_{rd} of dielectric coating. Here, with the increasing value of gyromagnetic coupling the increase of difference between ferrite modes propagation coefficients is observed (see Fig. 6(f)).

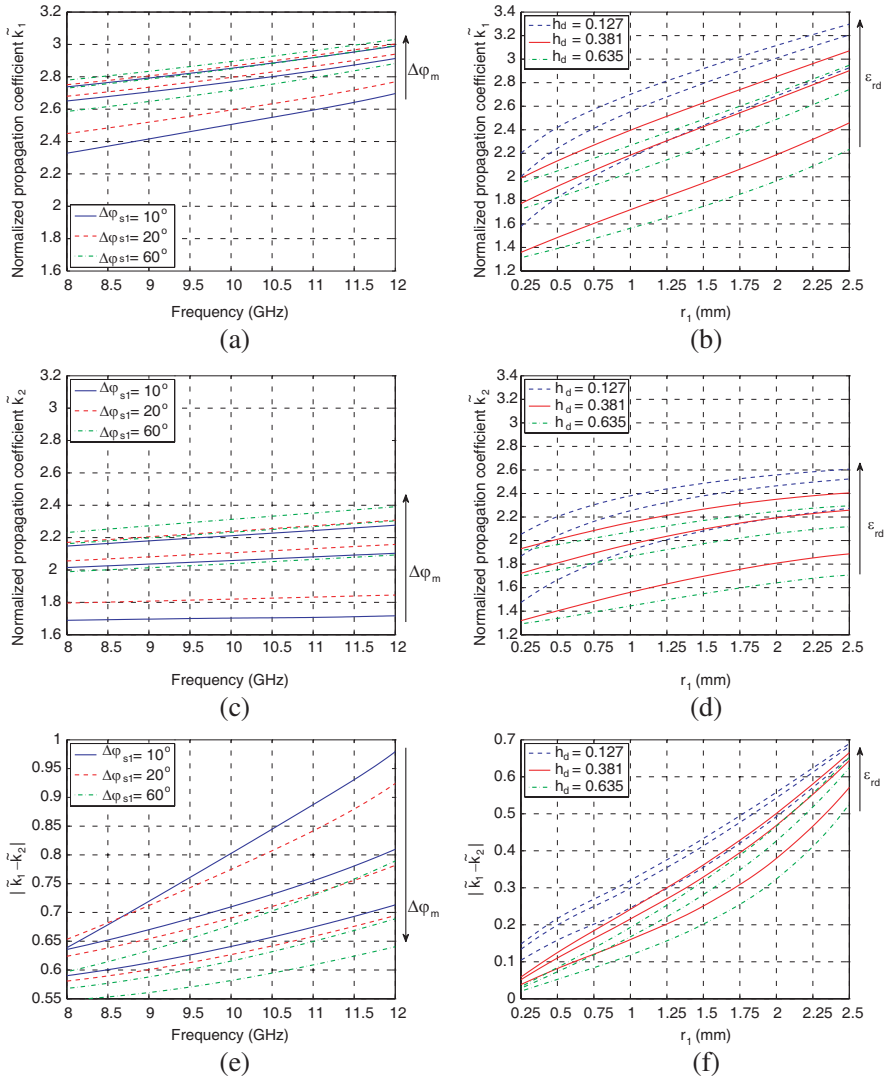

Figure 6. Characteristics of normalized propagation coefficients of two fundamental ferrite modes versus parameters of the guide from Fig. 5.

Finally, in Fig. 7 the parametric studies of ferrite section length L_{opt} ensuring Faraday rotation angle $\pi/4$ are presented. It can be noticed that according to the results obtained in Figs. 6(e) and 6(f) the length of the section L_{opt} increases with increasing $\Delta\varphi_{s1}$ and $\Delta\varphi_m$

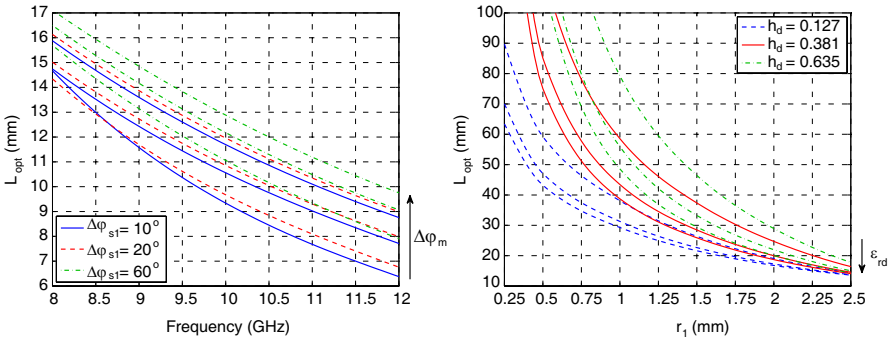

Figure 7. Characteristics of ferrite section length ensuring Faraday rotation angle $\pi/4$ versus parameters of the guide from Fig. 5.

for which the decrease of difference between ferrite modes propagation coefficients is observed. On the other hand the optimal length of the section becomes shorter when the height h_d and permittivity ε_r of dielectric coating are increasing.

3.2. Application of CFCL Junction to Circulator

In this section, the scattering parameters of circulator employing proposed CFCL junction are determined. The circulator is obtained by cascading T-junction and CFCL junction with Faraday rotation angle $\pi/4$. The required Faraday rotation angle is obtained when the CFCL junction satisfies amplitude and phase conditions [28]. For these conditions, the input signal is equally divided between two output ports of CFCL junction and the difference phase between output signals is equal 0 or 180°. In Section 3.2.1, the CFCL junction with the required amplitude and phase conditions is designed. Next, the scattering parameters of circulator are calculated by cascading S-parameters of ideal T-junction and the designed CFCL junction.

3.2.1. Scattering Parameters of CFCL Junction

Utilizing the results presented in Section 3.1 the CFCL junction satisfying amplitude and phase conditions for ensuring Faraday rotation angle $\pi/4$ is designed. In the analysis the center operation frequency $f_0 = 10\,\text{GHz}$ is assumed. The calculated scattering parameters of the junction for f_0 are shown in Fig. 8. From the presented results, it can be noticed that for length $L_{opt} = 12.94\,\text{mm}$ when one of the structure port is excited the signals are equally divided

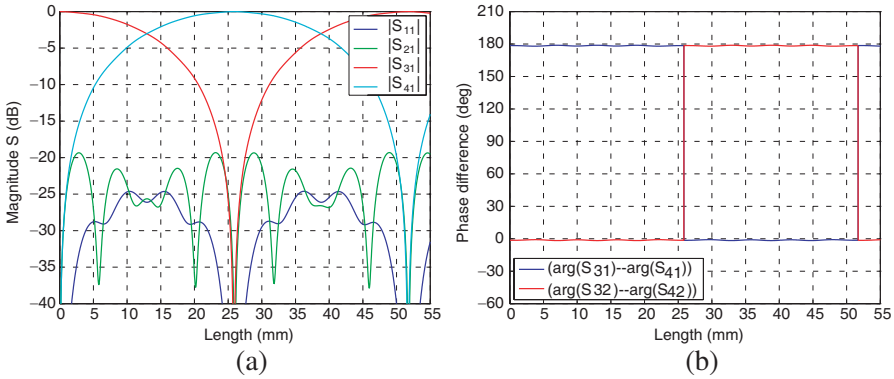

Figure 8. Length dependent scattering parameters characteristics of CFCL junction: (a) amplitude and (b) phase difference.

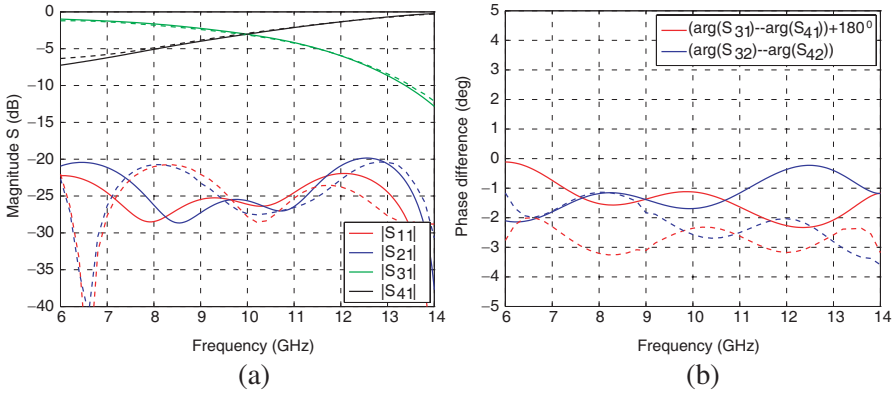

Figure 9. Frequency dependent scattering parameters characteristics of CFCL junction: (a) amplitude and (b) phase difference (solid line — MoM/CMM, dashed line — HFSS).

in the output ports. According to the phase difference the output signals are even and odd mode, respectively. Moreover, obtained L_{opt} is close to $L^a_{opt} = 12.92\,\text{mm}$ obtained from relation (33). For the considered section with $L_{opt} = 12.94\,\text{mm}$ the scattering parameters versus frequency are calculated and presented in Fig. 9. It can be found that $3 \pm 0.5\,\text{dB}$ power division is obtained in frequency range from 9.5 to 10.5 GHz. Moreover, the phase difference between output signals is varying from $-4°$ to 0 in the considered frequency range. The frequency dependent scattering parameters are compared with HFSS.

A good agreement of presented results with reference ones is observed.

3.2.2. Scattering Parameters of CFCL Circulator

Since, the CFCL junction from Section 3.2.1 satisfies required amplitude and phase conditions [28] it can be used in realization of nonreciprocal devices such as isolators, gyrators or circulators. This can be simply done by ensuring the proper excitation of CFCL junction. In Fig. 10, frequency response of single circulator obtained by cascading scattering parameters of ideal T-junction with calculated S-parameters of the investigated CFCL junction is presented. The investigated circulator with the following circulation direction $1 \rightarrow 3 \rightarrow 2 \rightarrow 1$ clearly shows nonreciprocal behavior. For this structure the isolation and reflection losses are better than -15 dB in frequency range from 8 to 11.5 GHz. In the simulation of the CFCL circulator parameters the lossless ferrite junction was assumed. Bearing in mind that the losses in FCL devices comes mainly from ferrite section we estimate their value in proposed junction with the use of commercial software HFSS. In the analysis the following material parameters were assumed for ferrite rod: resonance line width $\Delta H = 80$ Oe, $\tan\delta = 0.0005$, dielectric coating: $\tan\delta = 0.0009$ and metallization layers: $\sigma = 5.8e7$ S/m. For assumed parameters calculated losses were about 0.2 dB. Obtained results are much lower than insertion losses of coplanar FCL junction [15] operating in similar frequency range, for which the simulated in HFSS insertion losses were about

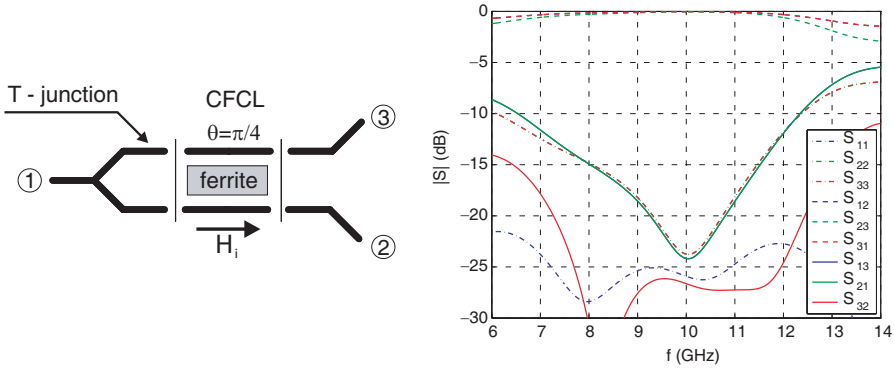

Figure 10. Frequency response of single circulator utilizing proposed CFCL junction from Fig. 1: (a) schematic view of the structure and (b) magnitude scattering parameters.

1.2 dB. Moreover, in comparison to [15] the length of the proposed ferrite section is about two times shorter, allowing for reduction of FCL devices dimensions.

4. CONCLUSION

In this paper, the novel cylindrical ferrite coupled line junction is presented. Utilizing the MoM/CMM approach the gyromagnetic coupling, dispersion characteristic and scattering parameters of CFCL junction are calculated. Obtained results show that in comparison to planar junctions in such section a higher gyromagnetic coupling occurs. This allows to use the ferrite materials with lower saturation magnetization and to reduce the length of the junction by a half. In result such CFCL junction exhibits much lower insertion losses and allows to reduce total dimensions of nonreciprocal devices in comparison to recently developed in literature planar FCL configurations.

ACKNOWLEDGMENT

This work was supported by Polish Ministry of Science and Higher Education from sources for science in the year 2011 under Contract No. 0215/T02/2010/70.

APPENDIX A.

In Equations (5)–(7) matrices $\mathbf{M}_{A1}^{E,l}$, $\mathbf{M}_{A1}^{H,l}$, $\mathbf{M}_{A2}^{E,l}$ and $\mathbf{M}_{A2}^{H,l}$ take the form

$$\mathbf{M}_{Ap}^{E} = \begin{bmatrix} \mathbf{M}_{Ap}^{E_z^e,l} & \mathbf{0} \\ \mathbf{M}_{Ap}^{E_\varphi^e,l} & \mathbf{M}_{Ap}^{E_\varphi^h,l} \end{bmatrix}, \tag{A1}$$

where

$$\mathbf{M}_{Ap}^{E_z^e,l} = \operatorname{diag}\left\{ R_m^{(p)}(k_{\rho l} r_l) \right\}_{m=-M}^{m=M}, \tag{A2}$$

$$\mathbf{M}_{Ap}^{E_\varphi^e,l} = \operatorname{diag}\left\{ \frac{-jm\gamma}{k_{\rho l}^2 r_l} R_m^{(p)}(k_{\rho l} r_l) \right\}_{m=-M}^{m=M}, \tag{A3}$$

$$2mm]\mathbf{M}_{Ap}^{E_\varphi^h,l} = \operatorname{diag}\left\{ -\frac{\omega\mu}{\eta k_{\rho l}} R_m'^{(p)}(k_{\rho l} r_l) \right\}_{m=-M}^{m=M} \tag{A4}$$

and

$$\mathbf{M}_{Ap}^{H,l} = \begin{bmatrix} \mathbf{0} & \mathbf{M}_{Ap}^{H_z^h,l} \\ \mathbf{M}_{Ap}^{H_\varphi^e,l} & \mathbf{M}_{Ap}^{H_\varphi^h,l} \end{bmatrix}, \tag{A5}$$

where

$$\mathbf{M}_{Ap}^{H_z^e,l} = \operatorname{diag}\left\{ \frac{j}{\eta_l} R_m^{(p)}(k_{\rho l} r_l) \right\}_{m=-M}^{m=M}, \tag{A6}$$

$$\mathbf{M}_{Ap}^{H_\varphi^e,l} = \operatorname{diag}\left\{ -\frac{j\omega\varepsilon}{k_{\rho l}} R_m^{\prime(p)}(k_{\rho l} r_l) \right\}_{m=-M}^{m=M}, \tag{A7}$$

$$\mathbf{M}_{Ap}^{H_\varphi^h,l} = \operatorname{diag}\left\{ \frac{m\gamma}{\eta_l k_{\rho l}^2 r_l} R_m^{(p)}(k_{\rho l} r_l) \right\}_{m=-M}^{m=M}. \tag{A8}$$

$p = \{1, 2\}$ and $R'_m(x) = \partial R_m(x)/\partial x$ denotes first derivative of Bessel function.

In Equations (12) and (17) matrices of integrals $\mathbf{I}_{os}$ and $\mathbf{I}_{so}$ take form:

$$\mathbf{I}_{os} = \operatorname{diag}\left\{ \mathbf{I}_{o,1}^s, \ldots, \mathbf{I}_{o,I}^s, \mathbf{I}_{o,0}^c, \mathbf{I}_{o,1}^c, \ldots, \mathbf{I}_{o,I}^c \right\} \tag{A9}$$

where

$$\left[\mathbf{I}_{os}^{s,i}\right]_{m,k} = \frac{1}{2\pi} \int_{\varphi_{si}}^{\varphi_{si}+\Delta\varphi_{si}} e^{-jm\varphi} \sin\left(\frac{\varphi - \varphi_{si}}{\Delta\varphi_{si}} k\pi \right), \tag{A10}$$

$$\left[\mathbf{I}_{os}^{c,i}\right]_{m,k} = \frac{1}{2\pi} \int_{\varphi_{si}}^{\varphi_{si}+\Delta\varphi_{si}} e^{-jm\varphi} \cos\left(\frac{\varphi - \varphi_{si}}{\Delta\varphi_{si}} k\pi \right) \tag{A11}$$

and

$$\mathbf{I}_{so} = 2\pi \left(\mathbf{I}_{os}^*\right)^{\mathrm{T}}. \tag{A12}$$

In Equation (17) matrices of electric field $\mathbf{M}^{E,2}$, $\mathbf{M}^{E,3}$ and magnetic field $\mathbf{M}^{H,2}$, $\mathbf{M}^{H,3}$ take the form

$$\mathbf{M}^{E,2} = \mathbf{M}_{A1}^{E,2} + \mathbf{M}_{A2}^{E,2}\mathbf{T}_{12}, \tag{A13}$$

$$\mathbf{M}^{H,2} = \mathbf{M}_{A1}^{H,2} + \mathbf{M}_{A2}^{H,2}\mathbf{T}_{12}, \tag{A14}$$

$$\mathbf{M}^{E,3} = \mathbf{M}_{A1}^{E,3}\mathbf{T}_{34} + \mathbf{M}_{A2}^{E,3}, \tag{A15}$$

$$\mathbf{M}^{E,3} = \mathbf{M}_{A1}^{E,3}\mathbf{T}_{34} + \mathbf{M}_{A2}^{E,3}. \tag{A16}$$

APPENDIX B.

In Equation (28) matrices **Q**, **k** and **K** take a form:

- matrix **Q**

$$\mathbf{Q} = \begin{bmatrix} 0 & 0 & Q_{1p} & Q_{1m}+Q_3 \\ 0 & 0 & Q_{1m}-Q_3 & Q_{1p} \\ Q_{2p} & Q_{2m} & 0 & 0 \\ Q_{2m} & Q_{2p} & 0 & 0 \end{bmatrix}, \tag{B1}$$

where $Q_{1p} = \frac{\beta_e Z_e + \beta_o Z_o}{2}$, $Q_{1m} = \frac{\beta_e Z_e - \beta_o Z_o}{2}$, $Q_{2p} = \frac{\beta_e Y_e + \beta_o Y_o}{2}$, $Q_{2m} = \frac{\beta_e Y_e - \beta_o Y_o}{2}$, $Q_3 = -\mathrm{j}C_{eo}$,

- matrix of eigenvalues **k**

$$\mathbf{k} = \mathrm{diag}\left\{k_1, -k_1, k_2, -k_2\right\}, \tag{B2}$$

where $k_1 = \sqrt{\beta_0^2 + \Gamma^2}$, $k_2 = \sqrt{\beta_0^2 - \Gamma^2}$, $\beta_0 = \sqrt{\frac{\beta_e^2+\beta_o^2}{2}}$, $\Delta\beta = \frac{\beta_e^2-\beta_o^2}{2}$ and $\Gamma^2 = \sqrt{\Delta\beta^2 + \frac{C_{eo}^2}{Z_e Z_o}\beta_e\beta_o}$,

- matrix of eigenvectors **K**

$$\mathbf{K} = \begin{bmatrix} K_{eo} & K_{eo} & K_{oe} & K_{oe} \\ K_{eo}^* & K_{eo}^* & -K_{oe}^* & -K_{oe}^* \\ Y_{ee}K_{oe} & -Y_{ee}K_{oe} & Y_{oo}K_{eo} & -Y_{oo}K_{eo} \\ Y_{ee}K_{oe}^* & -Y_{ee}K_{oe}^* & Y_{oo}K_{eo}^* & -Y_{oo}K_{eo}^* \end{bmatrix}, \tag{B3}$$

where $K_{eo} = 1 + \mathrm{j}\frac{\left(\Delta\beta^2-\Gamma^2\right)}{C_{eo}\beta_o}\sqrt{\frac{Z_o}{Z_e}}$, $K_{oe} = 1 + \mathrm{j}\frac{\left(\Delta\beta^2-\Gamma^2\right)}{C_{eo}\beta_e}\sqrt{\frac{Z_e}{Z_o}}$, $Y_{ee} = \frac{\beta_e Y_e}{k_1}$ and $Y_{oo} = \frac{\beta_o Y_o}{k_2}$.

REFERENCES

1. Mazur, J. and M. Mrozowski, "On the mode coupling in longitudinally magnetized waveguiding structures," *IEEE Transactions on Microwave Theory and Techniques*, Vol. 37, No. 1, 159–164, Jan. 1989.
2. Queck, C. K. and L. E. Davis, "Microstrip and stripline ferrite-coupled-lines (FCL) circulators," *IEEE Transactions on Microwave Theory and Techniques*, Vol. 50, No. 12, 2910–2917, Dec. 2002.

3. Mazur, J., M. Mazur, and J. Michalski, "Coupled-mode design of ferrite-loaded coupled-microstrip-lines section," *IEEE Transactions on Microwave Theory and Techniques*, Vol. 50, No. 6, 1487–1494, Jun. 2002.
4. Cao, M., R. Pietig, H. C. Wu, and R. G. Gossink, "Perturbation theory approach to the ferrite coupled stripline," *Microwave Symposium Digest, 2004 IEEE MTT-S International*, Vol. 3, 1903–1906, May 2004.
5. Queck, C. K. and L. E. Davis, "Novel folding technique for planar ferrite-coupled-line circulators," *IEEE Transactions on Microwave Theory and Techniques*, Vol. 52, No. 5, 1369–1374, May 2004.
6. Queck, C. K. and L. E. Davis, "Broad-band three-port and four-port stripline ferrite coupled line circulators," *IEEE Transactions on Microwave Theory and Techniques*, Vol. 52, No. 2, 625–632, Feb. 2004.
7. Mazur, J., M. Solecka, R. Poltorak, and M. Mazur, "Theoretical and experimental treatment of a microstrip coupled ferrite line circulator," *IEE Proceedings — Microwaves, Antennas and Propagation*, Vol. 151, No. 6, 477–480, Dec. 2004.
8. Cao, M. and R. Pietig, "Ferrite coupled-line circulator with reduced length," *IEEE Transactions on Microwave Theory and Techniques*, Vol. 53, No. 8, 2572–2579, Aug. 2005.
9. Yang, L.-Y. and K. Xie, "Design and measurement of nonuniform ferrite coupled line circulator," *Journal of Electromagnetic Waves and Applications*, Vol. 25, No. 1, 131–145, 2011.
10. Marynowski, W., A. Kusiek, and J. Mazur, "Microstrip four-port circulator using a ferrite coupled line section," *AEU — International Journal of Electronics and Communications*, Vol. 63, No. 9, 801–808, Jul. 2008.
11. Michalski, J., M. Mazur, and J. Mazur, "Scattering in a section of ferrite coupled microstrip lines: Theory and application in nonreciprocal devices," *IEE Proceedings — Microwaves, Antennas and Propagation*, Vol. 149, No. 5–6, 286–290, Oct. /Dec. 2002.
12. Sajin, G. I., S. Simion, F. Craciunoiu, A. A. Muller, and A. C. Bunea, "CRLH CPW antenna on magnetically biased ferrite substrate," *Journal of Electromagnetic Waves and Applications*, Vol. 24, No. 5–6, 803–814, 2010.
13. Zahwe, O., B. Abdel Samad, B. Sauviac, J. P. Chatelon, M. F. Blanc-Mignon, J. J. Rousseau, M. Le Berre, and D. Givord, "Yig thin film used to miniaturize a coplanar junction circulator," *Journal of Electromagnetic Waves and Applications*, Vol. 24, No. 1, 25–32, 2010.

14. Abdalla, M. A. and Z. Hu, "Multi-band functional tunable LH impedance transformer," *Journal of Electromagnetic Waves and Applications*, Vol. 23, No. 1, 39–47, 2009.
15. Marynowski, W. and J. Mazur, "Study of nonreciprocal devices using three-strip ferrite coupled line," *Progress In Electromagnetics Research*, Vol. 118, 487–504, 2011.
16. Bahri, R., A. Abdipour, and G. Moradi, "Analysis and design of new active quasi circulator and circulators," *Progress In Electromagnetics Research*, Vol. 96, 377–395, 2009.
17. Marynowski, W., A. Kusiek, and J. Mazur, "Microstrip ferrite coupled line isolators," *XVI International Microwaves, Radar and Wireless Communications Conference*, Vol. 1, 342–345, Krakow, Poland, May 2006.
18. Marynowski, W. and J. Mazur, "Treatment of the three strip coplanar lines on the ferrite," *XVII International Microwaves, Radar and Wireless Communications Conference*, Vol. 1, 135–138, Wroclaw, Poland, May 2008.
19. Kusiek, A., W. Marynowski, and J. Mazur, "Investigations of the circulation effects in the structure using ferrite coupled slot-line section," *Microwave and Optical Technology Letters*, Vol. 49, No. 3, 692–696, Jan. 2007.
20. Mazur, J., M. Mazur, J. Michalski, and E. Sdek, "Isolator using a ferrite-coupled-lines gyrator," *IEE Proceedings — Microwaves, Antennas and Propagation,* Vol. 149, No. 5–6, 291–294, Oct./Dec. 2002.
21. Queck, C. K. and L. E. Davis, "Bandwidth and losses of 4-port ferrite coupled lines circulators," *Microwave Symposium Digest, 2002 IEEE MTT-S International*, Vol. 3, 1475–1478, 2002.
22. Abdalla, M. A. and Z. Hu, "On the study of left-handed coplanar waveguide coupler on ferrite substrate," *Progress In Electromagnetics Research Letters*, Vol. 1, 69–75, 2008.
23. Abdalla, M. A. and Z. Hu, "Compact tuneable single and dual mode ferrite left-handed coplanar waveguide coupled line couplers," *Microwaves, Antennas Propagation, IET*, Vol. 3, No. 4, 695–702, Jun. 2009.
24. Marynowski, W. and J. Mazur, "Three-strip ferrite circulator design based on coupled mode method," *2009 International Symposium on Antennas and Propagation (ISAP 2009)*, 205–208, Bangkok, Thailand, Oct. 2009.
25. Marynowski, W. and J. Mazur, "Investigations of the double isolator using three-strip ferrite coupled line," *15th Conference*

on Microwave Techniques, COMITE 2010, 73–76, Brno, Czech Republic, Apr. 2010.

26. Harrington, R. F., *Time-harmonic Electromagnetic Fields*, McGraw-Hill Book Company, Inc., New York, 1961.
27. Wu, T. X. and D. L. Jaggard, "A comprehensive study of discontinuities in chirowaveguides," *IEEE Transactions on Microwave Theory and Techniques*, Vol. 50, No. 10, 2320–2330, Oct. 2002.
28. Mazur, J. and M. Mrozowski, "Nonreciprocal operation of structures comprising a section of coupled ferrite lines with longitudinal magnetization direction," *IEEE Transactions on Microwave Theory and Techniques*, Vol. 37, No. 6, 1012–1019, Jun. 1989.